BIOCHEMISTRY
including biophysical chemistry & molecular biology

Article

pubs.acs.org/biochemistry

A Noncanonical Cysteine Protease USP1 Is Activated through Active Site Modulation by USP1-Associated Factor 1

Mark A. Villamil, Junjun Chen, Qin Liang, and Zhihao Zhuang*

Department of Chemistry and Biochemistry, 214A Drake Hall, University of Delaware, Newark, Delaware 19716, United States

Supporting Information

ABSTRACT: Ubiquitin-specific proteases (USPs) constitute the largest family of the human deubiquitinating enzymes. USP1 belongs to the cysteine protease family and contains a catalytic triad comprised of C90, H593, and D751. Notably, the catalytic activity of USP1 is stimulated through the formation of a tight complex with a WD40 repeat protein UAF1 (USP1-associated factor 1). Our kinetic analyses revealed a general base catalysis in USP1/UAF1, in contrast to an ion-pair mechanism as demonstrated for papain and cathepsin. The pK_a value of the catalytic cysteine was determined to be 8.67 ± 0.07 in a pH-dependent inactivation study of USP1/UAF1 by iodoacetamide. A normal solvent kinetic isotope effect of 2.8 for k_{cat} and 3.0 for k_{cat}/K_m was observed in the USP1/UAF1-catalyzed hydrolysis of ubiquitin−AMC substrate. Moreover, proton inventory analysis supported the transfer of a single solvent-derived proton in the transition state. Our study also revealed the molecular basis for the activation of USP1 by UAF1. Although the pK_a of the catalytic cysteine in USP1 and USP1/UAF1 was almost identical, the pK_a of the catalytic histidine in USP1/UAF1 was 0.43 pH unit lower than that in USP1, which facilitates general base catalysis at a neutral pH and contributes to the elevated catalytic efficiency. We ruled out that the higher catalytic efficiency is due to a tighter binding of ubiquitin. Our results support a regulatory mechanism in which UAF1 activates USP1 by modulating its active site conformation. This finding has a general implication for the regulation of USPs that form complex with partner proteins.

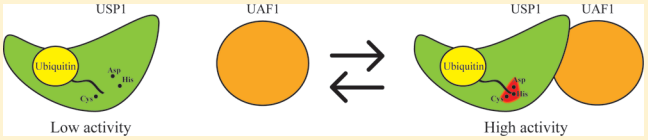

Deubiquitinating enzymes (DUBs) antagonize the ubiquitin ligase activity by removing the ubiquitin moiety from mono- or polyubiquitinated proteins. Abnormal cellular expression of DUBs or the loss of function due to mutation in certain DUB genes has been linked to various human diseases, including cancer as well as neurodegenerative and infectious diseases.[1−4]

Among the approximately 100 human DUBs, the ubiquitin-specific proteases constitute the largest DUB family with close to 60 members. USPs are usually large, multiple domain enzymes with a conserved catalytic core. The high-resolution structures of the catalytic core of several USPs revealed the conserved tripartite domain structures consisting of the palm, thumb, and finger domains.[5−8] An extended binding cleft for the ubiquitin C-terminal peptide is formed between the USP palm and thumb domains. The active site residues reside at the end of the cleft and are readily accessible to the solvent molecules in the apoenzyme structure. Besides the extensive interactions between the C-terminal tail of ubiquitin and the USP active-site cleft, the N-terminal face of ubiquitin also makes close contacts with the USP finger domain.

Multiple sequence alignment of USPs revealed two highly conserved active-site motifs, the Cys and His boxes, that contain the catalytic cysteine and histidine residues. In contrast, the third catalytic residue in the triad is not strictly conserved. In fact, USPs can be divided into separate groups depending on the identity of the third catalytic residue, such as Asp or Asn. As demonstrated by several high-resolution USP structures, a strictly conserved cysteine residue within the Cys box was found to reside at the N-terminal end of a central α-helix.[5−8] In the USP−ubiquitin complex structures, a highly conserved catalytic histidine residue in the His box is found within hydrogen-bond distance to the catalytic cysteine.[5,6,8] In contrast, the active site of some apo USP structures, such as USP7, is apparently in an unproductive conformation with the catalytic cysteine and histidine residues separated by more than 9 Å.[5]

USPs have been classified into the clan CA of papain-like protease.[9] On the basis of the conservation of the Cys, His, Asp/Asn catalytic triad, Storer and Menard suggested that the members in the CA clan of proteases share the catalytic mechanism of papain, in which the active site cysteine and histidine residues form a thiolate−imidazolium ion pair.[10] However, whether a thiolate−imidazolium ion pair mechanism operates in USPs has not been addressed previously.

There is growing evidence suggesting that the activity of DUBs, in particular USPs, is stringently regulated through their interaction with many other protein partners. USP1, a prototypical USP, is an inefficient enzyme alone. Upon formation of a complex with USP1-associated factor 1 (UAF1), the catalytic activity of USP1 is largely increased. UAF1 is a WD40 repeat protein that adopts an eight-bladed β-propeller structure.[11] Remarkably, a number of WD40 repeat

Received: January 12, 2012
Revised: March 5, 2012
Published: March 22, 2012

   dx.doi.org/10.1021/bi3000512 | *Biochemistry* 2012, 51, 2829−2839

proteins have been found to interact with human and yeast USPs.[12−14] Given its widespread occurrence, the interaction between WD40 repeat proteins and USPs likely represents a fundamentally important mechanism of regulating USP activity. To date, how USP1's catalytic activity is stimulated through interaction with UAF1 remains unclear. To investigate the possible mechanism of USP1 activation by UAF1, we employed the cysteine and histidine-reactive molecules, iodoacetamide and diethylpyrocarbonate, to determine the reactivity of the catalytic cysteine and histidine groups in the USP1/UAF1 complex or in USP1 alone. The pH dependence of the residue-specific modification of USP1/UAF1 or USP1 was determined. Coupled with the solvent kinetic isotope effect of USP1/UAF1 and USP1 in hydrolyzing Ub-AMC, we concluded that USP1/UAF1 catalyzes deubiquitination through a general base mechanism, which is distinctively different from the papain and cathepsin family proteases. Although the pK_a of the catalytic cysteine in USP1 and USP1/UAF1 was almost identical, the pK_a of the catalytic histidine in USP1/UAF1 was clearly different from that in USP1. Our results suggest a possible regulatory mechanism in which UAF1 activates USP1 through modulation of its active site conformation.

EXPERIMENTAL PROCEDURES

Expression and Purification of USP1/UAF1 and USP1. USP1 and UAF1 genes were cloned into pFastBac HT vector (Invitrogen) for insect cell (Sf9) expression.[15] To prevent proteolytic cleavage, GG670,671AA was introduced into the USP1 gene as reported.[15,16] The wild-type and mutant human USP1/UAF1 was expressed and purified as previously reported.[15] Specifically infected Sf9 cells were harvested 72 h postinfection. The cell pellet was washed twice with the PBS buffer containing 137 mM NaCl, 2.7 mM KCl, 10 mM Na_2HPO_4, 2 mM KH_2PO_4, pH 7.4. Cells were resuspended in the lysis buffer containing 50 mM NaH_2PO_4 (pH 8.0), 500 mM NaCl, 10 mM imidazole, 5 mM β-ME, and 10% glycerol. The resuspended cells were sonicated on ice and centrifuged at 4 °C. The supernatant was incubated with Ni-NTA agarose resin (Invitrogen) at 4 °C for 1 h with constant shaking and then washed with the lysis buffer extensively. The USP1/UAF1 complex was eluted from the resin with a buffer containing 50 mM NaH_2PO_4 (pH 8.0), 500 mM NaCl, 250 mM imidazole, 5 mM β-ME, and 10% glycerol. The purified protein complex contained a close to 1:1 stoichiometry of the USP1 and UAF1 subunits.[15] Protein purity was above 90% as judged by SDS-PAGE gel analysis (Figure S1). The desired fractions were combined and subjected to buffer exchange in the storage buffer containing 50 mM Tris (pH 8.0), 100 mM NaCl, 2 mM DTT, and 10% glycerol. The expression and purification of USP1 was carried out following the same protocol described for USP1/UAF1. Protein purity was analyzed by SDS-PAGE gel analysis, and the fractions with above 90% purity (Figure S1) were combined and subjected to buffer exchange in storage buffer containing 50 mM Tris (pH 8.0), 100 mM NaCl, 2 mM DTT, and 10% glycerol.

Steady-State Kinetic Measurement. The *in vitro* deubiquitinating activity of USP1 or USP1/UAF1 was assayed using a fluorogenic substrate ubiquitin 7-amino-4-methylcoumarin (Ub-AMC) (Enzo Life Sciences). Ub-AMC was incubated in a reaction buffer containing 50 mM HEPES (pH 7.8), 0.5 mM EDTA, 0.1 mg/mL BSA, and 1 mM DTT at 25 °C. The fluorescence signal was measured using a Fluoromax-4 fluorescence spectrophotometer (Horiba) following the addition of enzyme using an excitation wavelength of 355 nm and an emission at 440 nm. The initial rate was plotted against the substrate concentration ranging from 100 nM to 3 μM. The steady-state rate constant was determined by fitting the initial rates to the Michaelis−Menten equation $V = (V_{max}[S])/([S] + K_m)$ using GraphPad Prism (GraphPad Software, La Jolla, CA). The k_{cat} was determined by dividing the V_{max} with the total enzyme concentration used in the assay.

The steady-state kinetics of USP1/UAF1 hydrolyzing Ub-AMC in the presence of increasing concentrations of NaCl was measured in a buffer containing 50 mM HEPES (pH 7.8), 0.5 mM EDTA, 0.1 mg/mL BSA, 1 mM DTT, and the varying NaCl concentrations. The steady-state rate constants (k_{cat} and k_{cat}/K_m) were determined as described above and plotted against increasing NaCl concentrations.

Determine the Competitive Inhibition Constant of Methylergonovine Maleate. The inhibition of USP1/UAF1 and USP1 by methylergonovine maleate was determined in reactions containing 2 nM USP1/UAF1 or 15 nM USP1, 100−2600 nM Ub-AMC, and methylergonovine maleate of varied concentrations. The assay buffer contained 50 mM HEPES (pH 7.8), 0.5 mM EDTA, 0.1 mg/mL BSA, and 1 mM DTT. The Lineweaver−Burk plot was obtained by plotting $1/v$ against 1/[Ub-AMC] at different inhibitor concentrations (100−800 nM). For competitive inhibition, K_i was determined by fitting the data to eq 1 using Origin 8 (OriginLab Corp., Northampton, MA).

$$\frac{1}{v} = \frac{K_m}{V_{max}}\left(\frac{1}{[S]}\right)\left(1 + \frac{[I]}{K_i}\right) + \frac{1}{V_{max}} \quad (1)$$

$$\text{slope} = \frac{K_m}{V_{max}}\left(1 + \frac{[I]}{K_i}\right)$$

$$\text{intercept} = \frac{1}{V_{max}}$$

Protection of USP1/UAF1 and USP1 by Competitive Inhibitor. The reaction contained 40 nM USP1/UAF1 or 40 nM USP1, 6 mM iodoacetamide, and methylergonovine maleate (0.05−10 μM) in a buffer of 50 mM HEPES (pH 7.8), 0.5 mM EDTA, 0.1 mg/mL BSA, and 1 mM DTT. The assay mixture was incubated at 25 °C for 4 min, and then 150 nM Ub-AMC was added and the rate was determined by following the fluorescence at 440 nm with a 355 nm excitation. A similar experiment was performed with diethylpyrocarbonate (DEPC). The reaction contained 100 nM USP1/UAF1 or 100 nM USP1, 8 mM DEPC, and methylergonovine maleate (0.05−10 μM) in a buffer of 50 mM MOPS (pH 7.8), 0.5 mM EDTA, 0.1 mg/mL BSA, and 1 mM DTT. 200 nM Ub-AMC was added, and the reaction rate was determined as described above. A corresponding set of reaction solutions without iodoacetamide or DEPC were used as a control. The percent remaining activity was determined by taking the ratio of the rate with iodoacetamide or DEPC over its respective control. The percent enzyme activity remaining was plotted against the concentration of methylergonovine maleate and fitted to eq 2.

$$v = \frac{v_0[X]}{K_d + [X]} \quad (2)$$

pH Dependence of the Inactivation Rate of USP1/UAF1 and USP1 by Iodoacetamide. USP1/UAF1 (208

dx.doi.org/10.1021/bi3000512 | *Biochemistry* 2012, 51, 2829−2839

nM) or USP1 (300 nM) was incubated at 25 °C with various concentrations of iodoacetamide (0.5−8 mM) in a buffer containing 25 mM NaOAc, 25 mM MES, 25 mM glycine, 75 mM Tris, 0.1 mg/mL BSA, and 1 mM DTT with pH ranging from 5.6 to 10.6. The stability of the enzyme at the acidic and basic pHs was verified by carrying out preincubation tests. In the inactivation assay, aliquots of the preincubation mixture were diluted into a reaction mixture containing 200 nM Ub-AMC in 50 mM HEPES (pH 7.8), 0.5 mM EDTA, 1 mM DTT, and 0.1 mg/mL BSA at the various time points between 0 and 20 min. Release of AMC (7-amino-4-methylcoumarin) was monitored by fluorescence at an excitation wavelength of 355 nm and an emission wavelength of 440 nm. For each pH, the remaining USP1/UAF1 activity at the varied incubation time at a given iodoacetamide concentration was fitted to eq 3.

$$\text{remaining activity (\%)} = 100 \times \exp(-k_{obs}t) + C \quad (3)$$

The observed pseudo-first-order inactivation rate constant, k_{obs}, was plotted against the concentration of iodoacetamide. The second-order inactivation rate constant, k_2, was obtained from the slope of the resulting linear plot.[17] The profile of $\log(k_2)$ versus pH was fitted to eq 4[18] using GraphPad Prism 5 (GraphPad Software).

$$\log Y = \log \frac{Y_L + Y_H \times 10^{pH-pK_a}}{1 + 10^{pH-pK_a}} \quad (4)$$

where Y is k_2, and Y_L and Y_H are the minimum and maximum values of k_2, respectively.

pH Dependence of the Inactivation Rate of USP1/UAF1 and USP1 by Diethylpyrocarbonate. USP1/UAF1 (200 nM) or USP1 (300 nM) was incubated at 25 °C with varying concentrations of diethylpyrocarbonate (DEPC) (0.5−10 mM) in a buffer containing 50 mM MOPS, 50 mM MES, 50 mM Bicine, 0.1 mg/mL BSA, and 1 mM DTT with pH ranging from 5.6 to 9.6. The procedure was similar to the inactivation assay with iodoacetamide. The remaining activity of USP1/UAF1 or USP1 was fitted to eq 3. The observed pseudo-first-order inactivation rate constant, k_{obs}, was plotted against the concentration of diethylpyrocarbonate, and the second-order rate constant k_2 was obtained from the slope of the resulting linear plot. The profile of $\log(k_2)$ versus pH was fitted to eq 4 using GraphPad Prism 5 (GraphPad Software).

Solvent Kinetic Isotope Effect of USP1/UAF1 Catalyzed Ub-AMC Hydrolysis. The k_{cat} and k_{cat}/K_m pH profiles for the catalyzed hydrolysis of Ub-AMC by USP1/UAF1 were measured using a mixed buffer system consisting of 25 mM NaOAc, 25 mM MES, 25 mM glycine, 75 mM Tris, 0.1 mg/mL BSA, and 1 mM DTT with pH values ranging from 5.6 to 10.6. The stability of the enzymes at the acidic and basic pH values was verified by carrying out preincubation tests. The k_{cat} and k_{cat}/K_m values measured as a function of the assay solution pH were analyzed using eq 5 and GraphPad Prism 5 (GraphPad Software).

$$\log Y = \log \frac{C}{1 + 10^{pK_{a1}-pH} + 10^{pH-pK_{a2}}} \quad (5)$$

Y is the observed value of either k_{cat}/K_m or k_{cat}, and C is the pH-independent plateau value of Y. The pD profile was determined in the same manner in D_2O buffer. The pD values of the buffer were adjusted with DCl and NaOD, and the values of pD were determined as $pD = pH_{measured} + 0.40$. The pH(D)-independent value C for the pH and pD profiles were used to determine the sKIE for k_{cat} and k_{cat}/K_m.

The k_{cat} and k_{cat}/K_m pH profiles for the catalyzed hydrolysis of Ub-AMC by USP1 in H_2O buffer were measured as described for USP1/UAF1. However, the same measurement for USP1 in D_2O buffer was not pursued due to the extreme low level of activity of USP1 in D_2O buffer.

Proton Inventory Analysis. The assay was performed as described above in an assay buffer of pL 7.5 with varying deuterium atom fraction (n = 0−1) by mixing the appropriate volumes of protium oxide and deuterium oxide buffers. The ratio of k_{cat} measured in the protium oxide/deuterium oxide mixture relative to the k_{cat} determined in the protium oxide buffer was plotted against the deuterium atom fraction (n). The linearity of the plot was evaluated using a linear regression analysis.

Determine the Competitive Inhibition Constant of Ubiquitin. The inhibition of USP1/UAF1 and USP1 by ubiquitin was determined in reactions containing 2 nM USP1/UAF1 or 15 nM USP1, 100−2600 nM Ub-AMC, and ubiquitin at varied concentrations in a buffer containing 50 mM HEPES (pH 7.8), 0.5 mM EDTA, 0.1 mg/mL BSA, and 1 mM DTT. The Lineweaver−Burk plot was obtained by plotting $1/v$ against 1/[Ub-AMC] at different inhibitor concentrations (1.5−4 μM). For competitive inhibition, K_i was determined by fitting the data to eq 1 using Origin 8 (OriginLab Corp., Northampton, MA).

Progress Curve Analysis of the Inhibition of USP1/UAF1 and USP1 by Ub-aldehyde. The progress curve of the USP1/UAF1 (10 nM) or USP1 (10 nM) catalyzed hydrolysis of Ub-AMC (1000 nM) in the presence of inhibitor Ub-aldehyde (Boston Biochem) was obtained in a buffer containing 50 mM HEPES (pH 7.8), 0.5 mM EDTA, 0.1 mg/mL BSA, and 1 mM DTT. The range of Ub-aldehyde concentrations was 5−640 nM for USP1/UAF1 and 10−1280 nM for USP1 alone. The reaction was allowed for 5 min for USP1/UAF1 and 15 min for USP1 alone. The progress curve was fitted to eq 6

$$y = A_0 + A_1 e^{-k_{obs}t} \quad (6)$$

where k_{obs} is the observed inhibitory rate constant obtained for each inhibitor concentration. The k_{obs} was plotted against the corresponding Ub-aldehyde concentration [I] and fitted to eq 7[19]

$$k_{obs} = \frac{k_i[I]}{[I] + K_{in}\left(1 + \frac{[S]}{K_m}\right)} \quad (7)$$

where [S] is the substrate concentration, k_i is the second-order inhibition constant, and K_{in} is the equilibrium dissociation constant of Ub-aldehyde.

RESULTS

Mutational Analysis of the Catalytic Residues in USP1/UAF1. The enzymatic activity of USP1 alone, or the USP1/UAF1 complex, was assayed using a fluorogenic ubiquitin substrate, Ub-AMC, in which the C-terminus of ubiquitin is derivatized with 7-amino-4-methylcoumarin (AMC). Cleavage of the AMC group from ubiquitin resulted in the increase of fluorescence intensity at 440 nm upon excitation at 355 nm. With this assay, we obtained steady-state enzyme kinetic rate constants for USP1 and USP1/UAF1 at pH

dx.doi.org/10.1021/bi3000512 | Biochemistry 2012, 51, 2829−2839

7.8. The initial velocities were determined at varied Ub-AMC concentrations that ranged from 100 nM to 3 μM. The data were fit to the Michaelis–Menten equation to obtain k_{cat} and K_m. USP1 alone showed a low level of activity (k_{cat} = 0.004 s^{-1}, K_m = 0.57 μM, k_{cat}/K_m = 7.0 × 10^3 M^{-1} s^{-1}). The USP1/UAF1 complex demonstrated a 36-fold increase in catalytic efficiency as judged by k_{cat}/K_m (k_{cat} = 0.096 s^{-1}, K_m = 0.38 μM, k_{cat}/K_m = 2.5 × 10^5 M^{-1} s^{-1}). Our results are in accord with an earlier report of the copurified USP1/UAF1 complex.[11]

Ubiquitin-specific proteases contain conserved Cys, His, and Asp/Asn residues that form a potential catalytic triad. Based on the multiple sequence alignment of the catalytic core of a group of USPs that share sequence similarity to USP1, the potential USP1 catalytic triad residues, C90, H593, and D751, were identified (Figure S2). To confirm the identity of the catalytic residues, we first mutated C90 to either Ser or Ala. USP1(C90S)/UAF1 demonstrated a 714-fold decrease in catalytic efficiency as judged by k_{cat}/K_m (Table 1). No activity

Table 1. Steady-State Kinetic Properties of Wild-Type and Mutant USP1/UAF1

enzyme	k_{cat} (s^{-1})	K_m (nM)	k_{cat}/K_m (M^{-1} s^{-1})
USP1	(4.0 ± 0.2) × 10^{-3}	570 ± 70	7.0 × 10^3
USP1/UAF1 (WT)	(9.6 ± 0.5) × 10^{-2}	380 ± 130	2.5 × 10^5
USP1(C90S)/UAF1	(2.9 ± 0.2) × 10^{-4}	830 ± 180	350
USP1(C90A)/UAF1	no activity		
USP1(H593Q)/UAF1	no activity		
USP1(D751A)/UAF1	(1.2 ± 0.1) × 10^{-4}	740 ± 110	160

was detected for USP1(C90A)/UAF1, confirming the essential role of C90 in catalysis. Remarkably, USP1(H593Q)/UAF1 was inactive under the assay condition containing up to 100 nM enzyme and 500 nM Ub-AMC as a substrate. A third catalytic residue Asp751 was also evaluated by mutation. The catalytic efficiency of the USP1(D751A)/UAF1 was reduced as compared to the wild-type enzyme albeit to a lesser extent than the mutants of the other two catalytic triad residues (1560-fold decrease in k_{cat}/K_m) (Table 1).

Stability of USP1/UAF1 in Varying NaCl Concentrations. The steady-state kinetic parameters for USP1/UAF1-catalyzed hydrolysis of Ub-AMC were determined at NaCl concentrations ranging from 0.05 to 1 M. At each NaCl concentration the initial velocity was determined at various Ub-AMC concentrations that ranged from 100 nM to 3 μM. In all NaCl concentrations the data could be fit to the Michaelis–Menten equation to obtain the steady-state kinetic constants, k_{cat} and K_m. In Figure 1, the k_{cat} and K_m values were plotted against the salt concentrations. We observed a modest 2-fold decrease in k_{cat} values when the salt concentrations were increased from 50 mM to 1 M. Given that USP1 alone is 24-fold lower in k_{cat} (Table 1), we concluded that USP1/UAF1 complex is largely stable even in the presence of high salt concentration. The K_m values increase with a linear dependence on NaCl concentration (a 3.5-fold increase from 50 mM to 1 M NaCl) (Figure 1).

pH Dependence of Inactivation of USP1/UAF1 and USP1 by Iodoacetamide. Our mutational study confirmed C90 as the catalytic residue in USP1. The reactivity of the catalytic cysteine thiol group in USP1/UAF1 was investigated

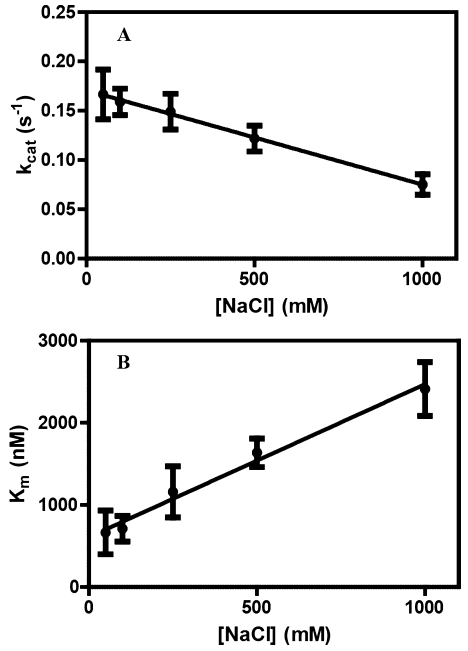

Figure 1. Dependence of the steady-state kinetic parameters of USP1/UAF1 on the concentration of NaCl. The k_{cat} and K_m values determined from initial velocities using Ub-AMC as a substrate was plotted against the salt concentration.

by measuring the second-order rate constant of its inactivation by the alkylating agent iodoacetamide (IAM). To ensure that the inactivation of USP1/UAF1 by iodoacetamide is due to the modification of the active site cysteine, we first carried out inactivation reaction in the presence of increasing concentrations of a competitive inhibitor of USP1/UAF1, methylergonovine maleate, identified previously in a high throughput screening.[15] Methylergonovine maleate was shown to be a potent competitive inhibitor of USP1/UAF1 with a K_i of 75 nM (Figure S3). We found that titration of increasing concentrations of methylergonovine maleate into a solution containing USP1/UAF1 and iodoacetamide protected the enzyme from inactivation. As shown in Figure 2A, close to 100% remaining activity was obtained when 10 μM of the inhibitor was added, which supports the notion that the loss of activity of USP1/UAF1 following the treatment with iodoacetamide is due to the covalent modification of the active site cysteine.

Next we measured the pH dependence of the inactivation rate of USP1/UAF1 by iodoacetamide following protocols that have been described for several other enzymes containing a catalytically essential cysteine residue.[17,20−22] The pH dependence of USP1/UAF1 inactivation at 25 °C by iodoacetamide over the pH range of 5.6−10.6 is shown in Figure 3A. Fitting the sigmoid-shaped curve to eq 4 afforded a pK_a value of 8.67 ± 0.07. We assigned this pK_a to the catalytic cysteine in USP1/UAF1.

A similar experiment was carried out for USP1 alone at the pH range of 5.6−10.6. As in USP1/UAF1, high concentration of the competitive inhibitor methylergonovine maleate can effectively protect the USP1 active site from inactivation by iodoacetamide (Figure 2B). A similar sigmoid-shaped inhibition curve was observed for USP1 inactivation by iodoacetamide over the pH range tested (Figure 3A). The fitted pK_a value for

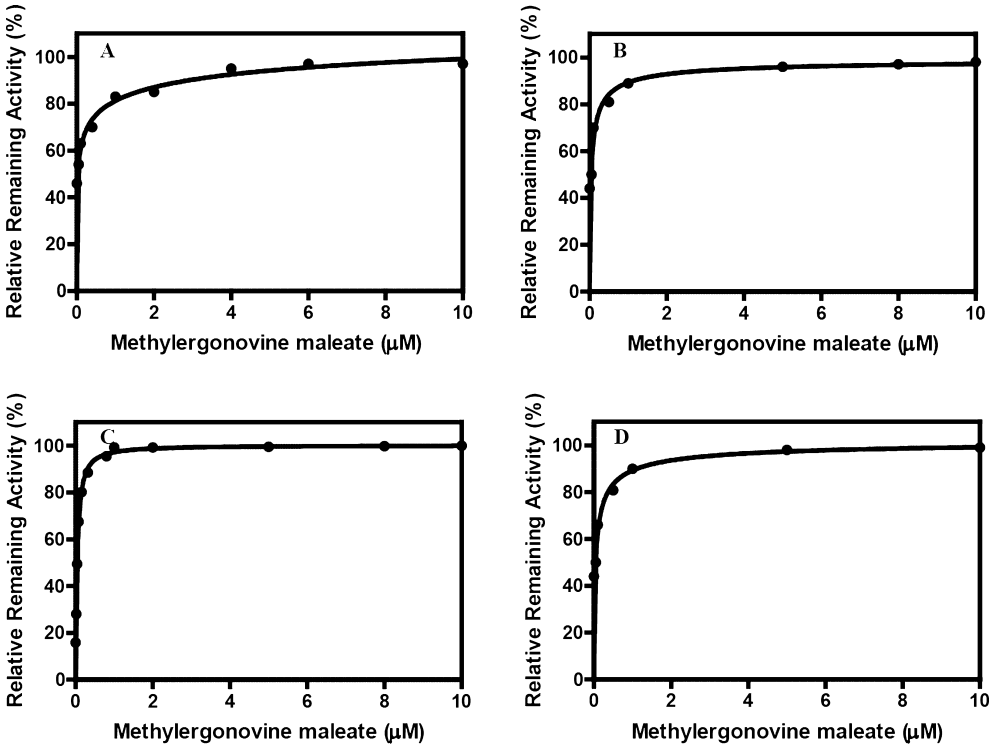

Figure 2. Protection of the active site cysteine of USP1/UAF1 (A) and USP1 (B) by methylergonovine maleate from inactivation by IAM. Protection of the active site histidine of USP1/UAF1 (C) and USP1 (D) by methylergonovine maleate from inactivation by DEPC.

USP1 is 8.71 ± 0.04. This observed value is very close to that observed for USP1/UAF1.

pH Dependence of Inactivation of USP1/UAF1 and USP1 by DEPC. Mutation of the USP1 His593 to Gln led to inactivation of USP1/UAF1, suggesting a critical role of His593 in catalysis. To probe the catalytic function of His593, we measured the second-order inactivation rate constant of USP1/UAF1 and USP1 by a histidine modifier diethylpyrocarbonate (DEPC).[23−26] Treatment of USP1/UAF1 by DEPC resulted in a large decrease in USP1/UAF1's catalytic activity (Figure S4). To confirm that the inactivation was due to the modification of the ω2 nitrogen of the histidine imidazole ring by carbethoxy group, we treated the inactivated USP1/UAF1 with 0.5 M hydroxylamine and found the USP1/UAF1 activity was largely recovered following the hydroxylamine treatment (Figure S4). Using the competitive inhibitor of USP1/UAF1, methylergonovine maleate, we confirmed that the loss of USP1/UAF1 activity was due to the modification of the active site histidine by DEPC (Figure 2C). We measured the pH dependence of the inactivation rate of USP1/UAF1 by DEPC. Similar to iodoacetamide as an inactivator, a sigmoidal curve was obtained for the inactivation of USP1/UAF1 by DEPC. Fitting the pH-dependent inactivation curve to eq 4 gave a pK_a value of 7.13 ± 0.05 (Figure 3B). This pK_a most likely derives from the ionization of the catalytic histidine in USP1/UAF1. A similar experiment was carried out for USP1 alone. We confirmed that DEPC inactivated USP1 specifically by modifying the catalytic histidine as demonstrated by the protection experiment using methylergonovine maleate (Figure 2D). A similar sigmoidal inactivation curve was observed with a calculated pK_a of 7.56 ± 0.08 (Figure 3B), which is 0.43 pH unit higher compared to that of USP1/UAF1.

Solvent Kinetic Isotope Effect of USP1/UAF1-Catalyzed Hydrolysis of Ub-AMC. To obtain a reliable solvent kinetic isotope effect (sKIE) of USP1/UAF1-catalyzed hydrolysis of Ub-AMC, we determined the pH(D) profile of the USP1/UAF1 complex in hydrolyzing Ub-AMC. We first

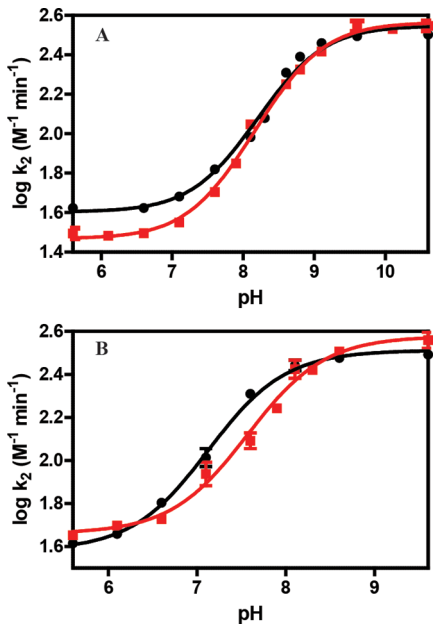

Figure 3. pH dependence of inactivation of USP1/UAF1 and USP1 by iodoacetamide (IAM) and diethylpyrocarbonate (DEPC). (A) log(k_2) measured for the inactivation of USP1/UAF1 (black circle) and USP1 (red square) by iodoacetamide versus pH was plotted and fitted to eq 4 to obtain the pK_a value of the catalytic cysteine residue. (B) log(k_2) measured for the inactivation of USP1/UAF1 (black circle) and USP1 (red square) by DEPC versus pH was plotted and fitted to eq 4 to obtain the pK_a value of the catalytic histidine residue.

dx.doi.org/10.1021/bi3000512 | *Biochemistry* 2012, 51, 2829−2839

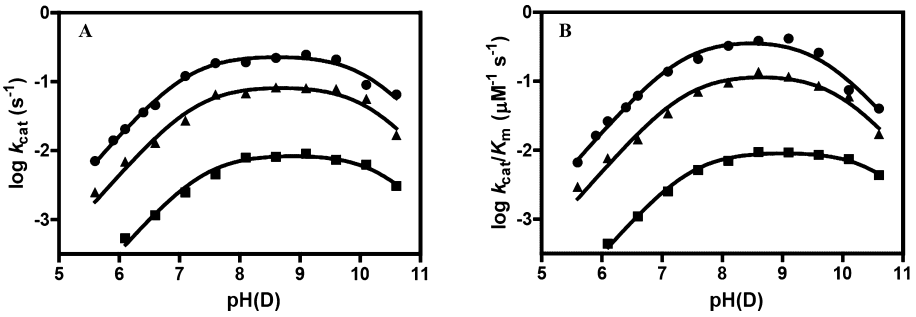

Figure 4. pH(D) dependence of USP1/UAF1 or USP1 in hydrolyzing Ub-AMC. (A) log(k_{cat}) pH(D) profile of USP1/UAF1 in H_2O (●) or in D_2O (▲) and log(k_{cat}) pH profile of USP1 in H_2O (■). (B) log(k_{cat}/K_m) pH(D) profile of USP1/UAF1 in H_2O (●) or in D_2O (▲) and log(k_{cat}/K_m) pH profile of USP1 in H_2O (■).

assessed whether USP1/UAF1 is stable over the pH range tested (pH 5.6−10.6). USP1/UAF1 was preincubated in buffer of different pHs, and then the enzymatic activity was determined in an assay buffer of pH 7.8. Incubation of USP1/UAF1 did not lead to loss of enzyme activity even at the extreme pHs of 5.6 and 10.6. The logarithm values of k_{cat} and k_{cat}/K_m were plotted against pH, and a bell-shaped profile was obtained in both cases between pH 5.6 and 10.6 (Figure 4). An increase in log(k_{cat}) value was observed between pH 5.6 and 7.6 with an observed slope of +1. A decrease in log(k_{cat}) was observed between pH 9.6 and 10.6 with an observed slope of −1. A plateau was observed between pH 7.6 and 9.6. Fitting the bell-shaped log(k_{cat}) pH profile to eq 5 afforded pK_{a1} of 7.15 ± 0.04 and pK_{a2} of 10.09 ± 0.08 with a pH-independent value of 0.25 ± 0.02 (see Table 2). The log(k_{cat}/K_m) pH profile was also bell-shaped and resembles that of the log(k_{cat}) pH profile. A close inspection revealed a narrower plateau region (pH 7.6−9.1) and a steeper decrease in the basic limb of the curve. Fitting the data to eq 5 led to pK_{a1} of 7.34 ± 0.08 and pK_{a2} of 9.62 ± 0.11 with a pH-independent value 0.39 ± 0.06 (Table 2).

Table 2. pK_a Values and Solvent Kinetic Isotope Effect of USPl/UAFl

solvent	pK_a value (k_{cat})	pK_a value (k_{cat}/K_m)	C value (k_{cat})	C value (k_{cat}/K_m)
H_2O	pK_{a1} = 7.15 ± 0.04	pK_{a1} = 7.34 ± 0.08	0.25 ± 0.02	0.39 ± 0.06
	pK_{a2} = 10.09 ± 0.08	pK_{a2} = 9.62 ± 0.11		
D_2O	pK_{a1} = 7.27 ± 0.11	pK_{a1} = 7.40 ± 0.20	0.09 ± 0.02	0.13 ± 0.03
	pK_{a2} = 10.10 ± 0.18	pK_{a2} = 9.89 ± 0.14		
sKIE			2.8	3.0

The pD profile for USP1/UAF1 hydrolyzing Ub-AMC was determined in 97% D_2O buffer. Both the log(k_{cat}/K_m) and log(k_{cat}) pD profiles are bell-shaped between pD 5.6 and 10.6 (Figure 4). Fitting the log (k_{cat}/K_m) profile to eq 5 yielded pK_a values of 7.40 ± 0.20 and 9.89 ± 0.14 with a pD-independent value of 0.13 ± 0.03. Similarly, fitting the log(k_{cat}) profile yielded pK_a values of 7.27 ± 0.11 and 10.10 ± 0.18 with a pD-independent value of 0.09 ± 0.02.

A decrease in catalytic efficiency was observed for USP1/UAF1-catalyzed hydrolysis of Ub-AMC in D_2O buffer. A normal solvent kinetic isotope effect was observed for both k_{cat} and k_{cat}/K_m. A sKIE of 2.8 for k_{cat} was calculated from the pH-independent values obtained from fitting the pH/D data to eq 5. A similar sKIE of 3.0 was also observed for k_{cat}/K_m by comparing the pH-independent values.

We also determined the steady-state kinetic parameters of k_{cat} and K_m for USP1-catalyzed hydrolysis of Ub-AMC at pH values ranging from 5.6 to 10.6. USP1 was shown to be stable within the range of pH tested by preincubating USP1 with the buffers of different pH, followed by activity assay in a buffer of pH 7.8. The log(k_{cat}) and log(k_{cat}/K_m) values were plotted against pH. We observed 27−44-fold reduction in the catalytic activity for USP1 at the various pH tested as compared to USP1/UAF1. The acidic limb of the pH profile is better defined with an observed slope of +1 for both log(k_{cat}) and log(k_{cat}/K_m) profiles. Fitting the log(k_{cat}) and log(k_{cat}/K_m) profiles yielded pK_a values of 7.40 ± 0.06 and 7.50 ± 0.04, respectively. Fitting the basic limb of the pH profile afforded pK_a values of 10.36 ± 0.11 and 10.55 ± 0.08 for the log(k_{cat}) and log(k_{cat}/K_m) profiles. It was not possible to determine the pD profile for USP1 due to the extremely low activity of USP1 in D_2O buffer.

Proton Inventory Study of USP1/UAF1-Catalyzed Ub-AMC Hydrolysis. A proton inventory study was performed on the USP1/UAF1 complex. The steady-state kinetic constant k_{cat} was measured as a function of the atom fraction of deuterium present in mixtures of protium oxide and deuterium oxide (0−99%) in the assay buffer.[27] The plot of $^{n}k_{cat}/^{0}k_{cat}$ versus the deuterium atom fraction (n) was clearly linear as judged by the linear regression analysis with a least-squares correlation coefficient of 0.98 (Figure 5). This observation suggests that the solvent kinetic isotope effect on the hydrolysis of Ub-AMC

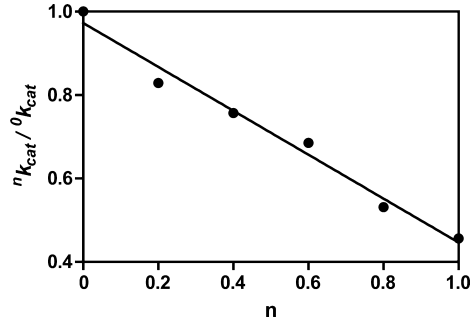

Figure 5. Proton inventory of USP1/UAF1-catalyzed hydrolysis of Ub-AMC. The ratio of k_{cat} measured in a buffer containing a mixture of D_2O and H_2O at varied deuterium atom fraction to that measured in 100% H_2O is plotted against the deuterium atom fraction (n). The data were collected at a pL of 7.8 at 25 °C. The data were analyzed using a linear regression analysis.

dx.doi.org/10.1021/bi3000512 | Biochemistry 2012, 51, 2829−2839

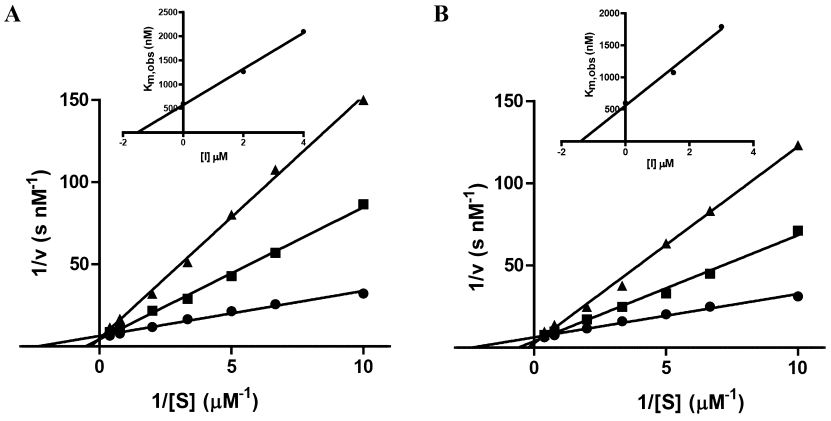

Figure 6. Inhibition of USP1/UAF1 and USP1 by ubiquitin. (A) Lineweaver–Burk plot of inhibition of USP1/UAF1 by 0 (●), 2 (■), and 4 (▲) μM ubiquitin. (B) Lineweaver–Burk plot of inhibition of USP1 by 0 (●), 1.5 (■), and 3 (▲) μM ubiquitin.

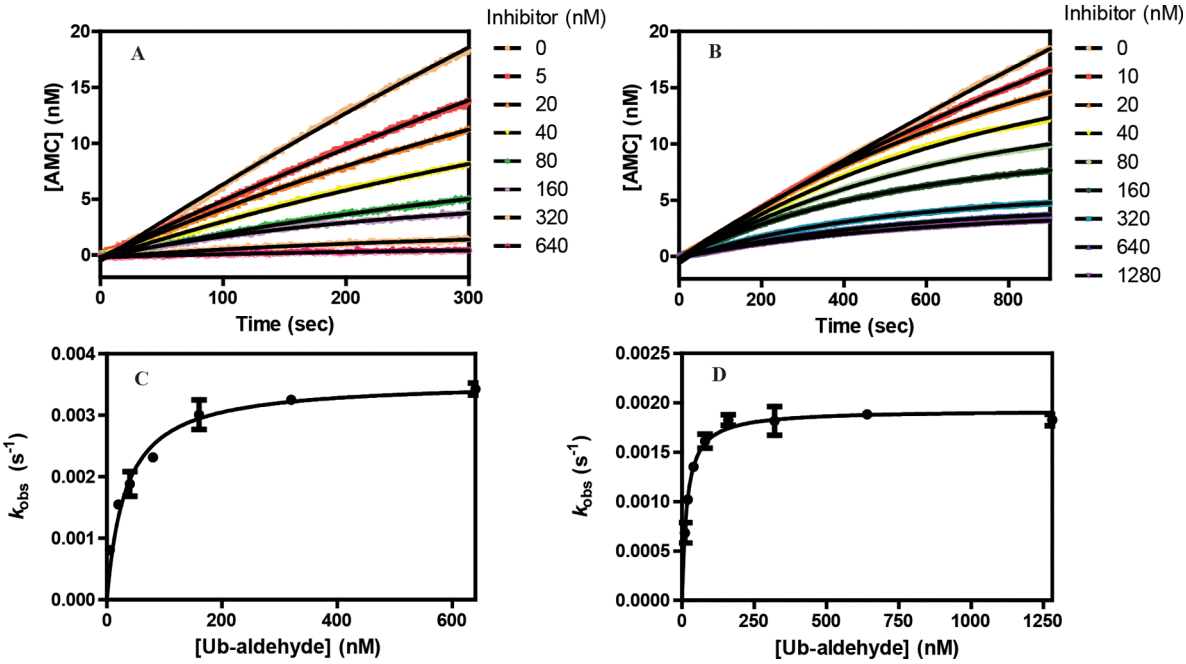

Figure 7. Progress curve analysis of inhibition of USP1/UAF1 and USP1 by Ub-aldehyde. Fitting the progress curves of inhibition of USP1/UAF1 (A) and USP1 (B) by Ub-aldehyde. Plots of the obtained k_{obs} versus [Ub-aldehyde] for USP1/UAF1 (C) and USP1 (D). Fitting of the plots to eq 7 allowed the determination of the second-order inhibition constant (k_i) and the equilibrium dissociation constant (K_{in}).

by USP1/UAF1 is due to the transfer of a single solvent-derived proton in the rate-limiting transition state.

Competitive Inhibition of USP1/UAF1 and USP1 by Ubiquitin. The available cocrystal structures of USP and ubiquitin showed a common mode of ubiquitin binding to the USP catalytic core. While the C-terminal peptide of ubiquitin binds to the catalytic cleft formed by the palm and thumb domains, interactions also exist between the ubiquitin N-terminal region and the finger domain. We found that ubiquitin is a competitive inhibitor of USP1/UAF1 with a measured K_i = 1.5 ± 0.4 μM (see Figure 6A). Ubiquitin also inhibits USP1 following a competitive mechanism with a K_i of 1.4 ± 0.3 μM (Figure 6B). These observations indicate that the association of UAF1 with USP1 does not change its binding affinity for ubiquitin.

Inhibition of USP1/UAF1 and USP1 by Ub-aldehyde. Ubiquitin-aldehyde (Ub-aldehyde) is a mechanism-based irreversible inhibitor of USPs.[28] A progress curve analysis was carried out for the inhibition of USP1/UAF1 and USP1 by Ub-aldehyde. The hydrolysis of Ub-AMC by USP1/UAF1 or USP1 was followed by fluorescence increase at 440 nm in the presence of a range of Ub-aldehyde concentrations. The progress curves were fitted to eq 6 to obtain the observed inactivation rate constant (Figure 7A,B). The obtained k_{obs} was then plotted against Ub-aldehyde concentration. Fitting the plot to eq 7 allowed the determination of the equilibrium dissociation constant for Ub-aldehyde (K_{in}) and the second-order inactivation rate constant (k_i) for USP1/UAF1 and USP1 (Figure 7C,D). A K_{in} of 16 ± 3 nM and a k_i of (3.6 ± 0.2) × 10^{-3} s^{-1} were obtained for USP1/UAF1; a K_{in} of 6.0 ± 0.7 nM and a k_i of (1.93 ± 0.04) × 10^{-3} s^{-1} were measured for USP1. The potency of Ub-aldehyde as an inhibitor of USP1/UAF1 and USP1 was very close as judged by k_i/K_{in} (2.2 × 10^5 M^{-1} s^{-1} for USP1/UAF1; 3.2 × 10^5 M^{-1} s^{-1} for USP1).

dx.doi.org/10.1021/bi3000512 | *Biochemistry* 2012, 51, 2829–2839

DISCUSSION

Ubiquitin is an 8.6 kDa protein, and its C-terminal glycine can be covalently conjugated to a target protein via an isopeptide bond. Ubiquitination requires a cascade of three enzymatic reactions to conjugate the ubiquitin moiety to the ε-amino group of a lysine side chain site specifically. Ubiquitin modification, like other essential forms of post-translational modification, is a dynamic, reversible process. The deubiquitinating enzymes (DUBs) are responsible for cleaving the isopeptide bond between ubiquitin and a target protein or between ubiquitin molecules within a polyubiquitin chain. The important cellular roles of DUBs are manifested by the large number of DUBs identified in eukaryotes. There are ~100 putative DUBs encoded by the human genome.[29] The human DUBs are highly divergent in their modular structures and primary sequences outside the enzymes' catalytic core.

To date, little is known about the physiological function of many DUBs, and the specific substrate of most DUBs remains elusive. DUBs belong to the protease superfamily and most DUBs are cysteine proteases. A small number of DUBs are metalloproteases.[29] Based on the sequence and fold of the catalytic core, DUBs are classified into five subclasses that are ubiquitin-specific protease (USP), ubiquitin C-terminal hydrolase (UCH), Otubain protease (OTU), Machado-Joseph disease protease (MJD), and JAB1/MPN/Mov34 metalloenzyme (JAMM). USPs constitute the largest DUB family and play a variety of important cellular functions.

USP1, a member of the USP family, is an enzyme involved in two essential DNA damage response pathways, i.e., the human translesion synthesis (TLS) and Fanconi anemia (FA) pathways. It represents an attractive target for the pharmacological modulation of both pathways.[15] The human USP1 is known to deubiquitinate PCNA and FANCD2, two essential proteins in eukaryotic DNA damage response.[11,16] It has been shown that monoubiquitination of PCNA is required for the successful translesion synthesis.[30−32] Monoubiquitination of PCNA recruits the TLS DNA polymerases to the stalled DNA replication fork for lesion-bypass synthesis. A deubiquitination step is likely required for restoring the normal DNA synthesis by the replicative DNA polymerases.[30,33] Human USP1 also deubiquitinates FANCD2 in the Fanconi anemia (FA) pathway.[34] A recent study in a chicken DT40 cell line showed that USP1 is indispensable for the cells' resistance to DNA damaging agents such as cisplatin and mitomycin C.[35] We recently identified USP1/UAF1-specific inhibitors that can sensitize human nonsmall cell lung cancer cells to DNA cross-linker cisplatin.[15] Disruption of USP1 function thus represents a promising therapeutic strategy for treating cancer.

The newly discovered role of UAF1 in up-regulating USP1's activity raised a new regulatory mechanism of USP by WD40 repeat protein.[11] Activation of USP1 activity by UAF1 can be achieved either directly through an interaction between the USP1 active site and UAF1, or indirectly through an allosteric mechanism, in which UAF1 binds to a region distant to the USP1 active site. Recently , the structure of a yeast ubiquitin-specific protease Ubp8, which is responsible for the deubiquitination of histone H2B, in complex with Sgf11 was reported.[36] The structure suggested that a direct contact between the USP active site and a motif in Sgf11 could organize the USP active site residues into a catalytically competent conformation.[36] In USP7 two terminal ubiquitin-like domains (ULDs) were found to interact with the enzyme catalytic site through the flexible C-terminal tail of USP7. This interaction leads to a conformational change in the so-called "switching loop" in the USP7 active site and realigns the active site into a productive conformation for catalysis.[37] Moreover, a partner protein GMP synthetase (GMPS) that interacts with USP7 and further stimulates its activity was thought to directly bind the first three ULDs in USP7 (HUBL-123) and promote an "on-state" in USP7, thus increasing its activity.[37] At present, little biochemical and structural information is available for the USP·WD40 repeat protein complex.

USP1 is a cysteine protease as suggested by the sequence alignment with a strictly conserved cysteine residue, Cys90, in the Cys box. Our mutational data support Cys90 as the catalytic cysteine in USP1. Interestingly, although mutation of Cys90 to Ser greatly reduced the catalytic efficiency, the mutant USP1(C90S)/UAF1 still retains significant activity in hydrolyzing Ub-AMC. In comparison, mutation of Cys90 to Ala completely abolished the activity of USP1/UAF1. Mutation of the catalytic triad His593 in USP1/UAF1 to Gln led to an inactive enzyme, which stresses the essential role of His593 in catalysis. Our mutation data suggested that the third catalytic triad residue Asp751 in USP1/UAF1 also contributes to catalysis but to a less extent. It was recently found that in USP2 mutation of the third catalytic triad residue Asn574 to Ala had little effect on the deubiquitination activity of USP2.[38] The difference in the contribution of the third catalytic residue to deubiquitination activity can be understood in view of the different identity of the third catalytic triad residue (Asp versus Asn). It is likely that the different charge state of the third catalytic residue may influence the catalytic mechanism of the cysteine triad in USPs. It should be noted that in two USPs, USP16 and USP30, the catalytic triad Asp/Asn is replaced by Ser.[29] Remarkably, USP16 and USP30 were shown to be active DUBs.[39−41] The variability in the third catalytic triad residue suggests that different catalytic mechanisms may operate in the USP active sites.

The papain-family proteases have been shown to form a Cys-S^-/His-ImH^+ ion pair in the free enzyme.[42] The thiolate of active site Cys acts as a nucleophile to attack the substrate's carbonyl group, which leads to a tetrahedral intermediate and subsequently the acyl-enzyme intermediate. In the deacylation step, a lytic water molecule serves as a nucleophile to attack the carbonyl group on the acyl-enzyme intermediate. This step results in the formation of the second tetrahedral intermediate, which then collapses to produce the product and also regenerates the free enzyme.[43] In papain, a pK_a value of 4.0 was reported for the active-site cysteine from pH-dependent inactivation of papain by chloroacetamide.[44] In a different study, a pK_a value of 3.7 for the papain active-site cysteine was obtained by measuring the absorbance change upon alkylation of active site cysteine with iodoacetamide.[42] Agreeing with the notion that a Cys-S^-/His-ImH^+ ion pair exists in the papain active site, no solvent kinetic isotope effect on the alkylation of papain active site cysteine by chloroacetamide was observed.[44] The unusual pK_a of cysteine was thought to be due to a nearby histidine residue which remains positively charged in pH up to 8.4.[45] In cathepsin C, an inverse solvent kinetic isotope effect of 0.71 was reported for k_{cat}/K_m. This observation agrees with an ion-pair mechanism in which the catalytic cysteine exists predominately in a thiolate form in the free enzyme and is poised for nucleophilic attack of the amide group in the peptide substrate.[46]

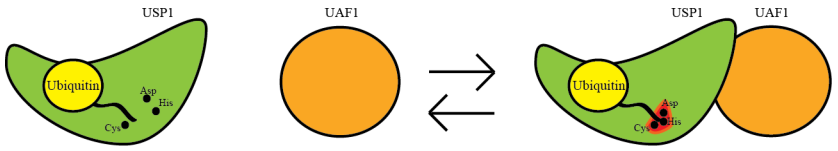

Figure 8. Illustration of the possible mechanism of activation of USP1 by UAF1 through an induced active-site conformation change.

Different from the papain family cysteine protease, the pK_a of the USP1/UAF1 catalytic cysteine thiol is largely unperturbed as determined by chemical modification of the active site cysteine by iodoacetamide. This observation argues against an ion-pair mechanism. Instead, a general base catalysis likely operates in USP1/UAF1. Agreeing with this notion, USP1/UAF1 displayed a normal solvent kinetic isotope effect on k_{cat} and k_{cat}/K_m (sKIE of 2.8 and 3.0, respectively), indicative of a general base catalysis in which a solvent kinetic isotope effect of 2−4 is expected.[45] Our proton inventory study showed that a single proton is transferred in the rate-limiting transition state. At present, it is not yet known which chemical step is the rate-limiting step in Ub-AMC hydrolysis. Further pre-steady-state kinetic analysis will be needed to address this question.

Several viral proteases have been proposed to follow general base catalysis. Poliovirus proteinase 3C (PV3C) belongs to the picornavirus family proteinases, which are structurally related to the trypsin family of serine peptidases.[47] Sarkany et al. reported a pK_a value of 9.1 and 8.55 for the active site cysteine when PV3C was treated with iodoacetamide and iodoacetate, respectively.[48] Thus, it was concluded that PV3C contains an active site thiol group with an unperturbed pK_a, which excludes the thiolate−imidazolium ion-pair mechanism. SARS 3C-like proteinase (SARS 3CL) was also suggested to utilize a general base mechanism for catalysis.[49] Huang et al. reported a pK_a of 8.34 for the active site Cys in SARS 3CL.[49] Further, a normal isotope effect around 1.3 was determined for k_{cat}/K_m.

In view of the catalytic mechanism, USP1 is more closely related to the viral proteinases despite that little structural similarity was observed between USPs and the poliovirus proteinase 3C and the SARS 3C-like proteinase. Interestingly, another viral protease, SARS-CoV PLpro, is likely evolutionarily related to USP given that a similar fold was found for the catalytic core of both proteases. Remarkably, the SARS-CoV PLpro was found to have a deubiquitinating activity.[50,51] It will be of interest to determine whether the SARS-CoV PLpro adopts a general base mechanism in deubiquitinating reaction.

USP1 alone is a highly inefficient enzyme with a k_{cat} of 0.004 s^{-1}. Upon forming a complex with UAF1, the deubiquitinating activity of USP1 is greatly stimulated. The mechanism underlying such stimulation has remained unclear. We compared the USP1/UAF1 complex to USP1 in the pH dependence of their inactivation by DEPC and iodoacetamide. The inactivation study of USP1/UAF1 by a histidine modifier DEPC revealed a pK_a of 7.13 for the catalytic histidine residue. In comparison, a similar DEPC inactivation study of USP1 alone revealed a pK_a value of 7.56, which is 0.43 pH unit higher than that of USP1/UAF1. The change in the pK_a of the catalytic histidine can be explained by the potential conformation change in the active site of USP1 upon association with UAF1. A unprotonated histidine serves the role as a general base more effectively in activating the catalytic cysteine thiol for nucleophilic attack of the amide bond as previously demonstrated for glyceraldehyde-3-phosphate dehydrogenase (GAPDH).[24] Notably, the pK_a of 7.13 for USP1/UAF1 catalytic histidine is still considerably higher than that of GAPDH (pK_a of 5.5). This may explain the relative low catalytic turnover number of USP1/UAF1 compared to GAPDH (k_{cat} of 0.096 s^{-1} versus 1056 s^{-1}). Likewise, a 24-fold lower k_{cat} can be attributed to a higher pK_a of the catalytic histidine in USP1 when compared to USP1/UAF1. In contrast to the catalytic histidine, the pK_a of the active site cysteine in USP1 and USP1/UAF1 are both close to 8.6. These observations argue that a general base catalysis operates in both USP1 and USP1/UAF1. The difference in the catalytic efficiency between the two active sites is likely due to the differences in the basicity of the catalytic triad histidine. It should be noted that despite being the most widely used DUB substrate, Ub-AMC is not a physiological substrate. It is possible that the nature of the substrate may affect the kinetic parameters of USP catalysis. Nonetheless, the allosteric mechanism of the activation of USP1 by UAF1 is likely conserved when different substrates are used.

Flexibility of the USP active site has been demonstrated previously for USP7. In the apo USP7 catalytic core structure, the distance between the catalytic Cys223 and His464 is too far for a hydrogen-bonding interaction.[5] Binding of an ubiquitin molecule helps to remodel the active site into an active conformation. More recently, it was found that the ubiquitin-like domains, HUBL-45, in the C-terminal region of USP7 promote a productive active site conformation through an interaction with a "switching loop" close to the USP7 active site.[37] Moreover, GMPS can bind and hyperactivate the full-length USP7 by promoting the productive active site conformation. Conformation flexibility of the cysteine catalytic triad has also been previously observed in other cysteine proteases, such as m-calpain. In the absence of the Ca^{2+} binding, the active site of m-calpain is distorted, resulting in an inactive enzyme. Binding of Ca^{2+} to m-calpain activates the protease by inducing conformation changes in the active site and bringing the catalytic triad cysteine and histidine residues within hydrogen bond distance.[52] This has been shown to be an important mechanism in modulating the cellular function of calpain. It is conceivable that UAF1 may regulate the USP1 deubiquitination activity by modulating the USP1 active site conformation. A UAF1-induced active site conformational change to realign the cysteine catalytic triad is an attractive possibility (see Figure 8) in light of the different pK_a values of the essential catalytic histidine residue in USP1 and the USP1/UAF1 complex.

The deubiquitinating activity of USP in principle can also be modulated through remodeling of the ubiquitin-binding site. As revealed by the apo USP14 structure, two surface loops, BL1 and BL2, cover the binding cleft for ubiquitin C-terminus.[8] Upon binding of ubiquitin, significant rearrangement of loops BL1 and BL2 widens the ubiquitin-binding cleft. It was proposed that the association of USP14 with the 26S proteasome may relieve the steric hindrance posed by the two surface loops and thus activate USP14.[8] However, we found that ubiquitin is an equally potent competitive inhibitor

dx.doi.org/10.1021/bi3000512 | *Biochemistry* 2012, 51, 2829−2839

of USP1/UAF1 and USP1, and the inactivation of USP1/UAF1 and USP1 by Ub-aldehyde showed similar efficiency. Thus, it is unlikely that Ub binding to USP1 is obstructed due to steric reasons. The observation that a similar K_m was determined for USP1 and USP1/UAF1 with Ub-AMC as a substrate also argued against this possibility. Thus, UAF1's association with USP1 most likely modulates the active site conformation and leads to a catalytically competent active site. In view that a large number of USPs were found to interact with WD40 repeat proteins,[12] the mechanism of activation uncovered in USP1/UAF1 may be of general importance in understanding the molecular mechanism of regulation of USPs by WD40 repeat proteins. Our findings also raised the potential of identifying allosteric or exosite inhibitors of USP1/UAF1 and other related USP complexes by targeting away from the USP active site. This represents an attractive strategy to achieve specificity of inhibiting the USP family enzymes. Indeed, in a recent high throughput screening against USP1/UAF1, we identified selective noncompetitive inhibitors.[15] In view that a large number of USPs function in a complex, a similar strategy can be adapted in finding inhibitors against other human USPs.

■ ASSOCIATED CONTENT

Ⓢ Supporting Information

Figures S1−S4. This material is available free of charge via the Internet at http://pubs.acs.org.

■ AUTHOR INFORMATION

Corresponding Author

*Phone: (302) 831-8940; e-mail: zzhuang@udel.edu.

Notes

The authors declare no competing financial interest.

■ ACKNOWLEDGMENTS

The authors gratefully acknowledge Paul F. Cook for helpful comments and suggestions on the analysis of the solvent kinetic isotope effect and the pH-dependent activity profile.

■ ABBREVIATIONS

DUB, deubiquitinating enzyme; USP, ubiquitin-specific protease; UAF1, USP1-associated factor 1; Ub-AMC, ubiquitin-7-amino-4-methylcoumarin; DEPC, diethylpyrocarbonate; GMPS, GMP synthetase; TLS, translesion synthesis; FA, Fanconi anemia.

■ REFERENCES

(1) Singhal, S., Taylor, M. C., and Baker, R. T. (2008) Deubiquitylating enzymes and disease. *BMC Biochem. 9* (Suppl 1), S3.

(2) Edelmann, M. J., and Kessler, B. M. (2008) Ubiquitin and ubiquitin-like specific proteases targeted by infectious pathogens: Emerging patterns and molecular principles. *Biochim. Biophys. Acta 1782*, 809−816.

(3) Yang, W. L., Zhang, X., and Lin, H. K. (2010) Emerging role of Lys-63 ubiquitination in protein kinase and phosphatase activation and cancer development. *Oncogene 29*, 4493−4503.

(4) Shanmugham, A., and Ovaa, H. (2008) DUBs and disease: activity assays for inhibitor development. *Curr. Opin. Drug Discovery Dev. 11*, 688−696.

(5) Hu, M., Li, P., Li, M., Li, W., Yao, T., Wu, J. W., Gu, W., Cohen, R. E., and Shi, Y. (2002) Crystal structure of a UBP-family deubiquitinating enzyme in isolation and in complex with ubiquitin aldehyde. *Cell 111*, 1041−1054.

(6) Renatus, M., Parrado, S. G., D'Arcy, A., Eidhoff, U., Gerhartz, B., Hassiepen, U., Pierrat, B., Riedl, R., Vinzenz, D., Worpenberg, S., and Kroemer, M. (2006) Structural basis of ubiquitin recognition by the deubiquitinating protease USP2. *Structure 14*, 1293−1302.

(7) Avvakumov, G. V., Walker, J. R., Xue, S., Finerty, P. J. Jr., Mackenzie, F., Newman, E. M., and Dhe-Paganon, S. (2006) Amino-terminal dimerization, NRDP1-rhodanese interaction, and inhibited catalytic domain conformation of the ubiquitin-specific protease 8 (USP8). *J. Biol. Chem. 281*, 38061−38070.

(8) Hu, M., Li, P., Song, L., Jeffrey, P. D., Chenova, T. A., Wilkinson, K. D., Cohen, R. E., and Shi, Y. (2005) Structure and mechanisms of the proteasome-associated deubiquitinating enzyme USP14. *EMBO J. 24*, 3747−3756.

(9) Rawlings, N. D., Tolle, D. P., and Barrett, A. J. (2004) MEROPS: the peptidase database. *Nucleic Acids Res. 32*, D160−164.

(10) Storer, A. C., and Menard, R. (1994) Catalytic mechanism in papain family of cysteine peptidases. *Methods Enzymol. 244*, 486−500.

(11) Cohn, M. A., Kowal, P., Yang, K., Haas, W., Huang, T. T., Gygi, S. P., and D'Andrea, A. D. (2007) A UAF1-containing multisubunit protein complex regulates the Fanconi anemia pathway. *Mol. Cell 28*, 786−797.

(12) Sowa, M. E., Bennett, E. J., Gygi, S. P., and Harper, J. W. (2009) Defining the human deubiquitinating enzyme interaction landscape. *Cell 138*, 389−403.

(13) Kee, Y., Yang, K., Cohn, M. A., Haas, W., Gygi, S. P., and D'Andrea, A. D. (2010) WDR20 regulates activity of the USP12 x UAF1 deubiquitinating enzyme complex. *J. Biol. Chem. 285*, 11252−11257.

(14) Bozza, W. P., and Zhuang, Z. (2011) Biochemical characterization of a multidomain deubiquitinating enzyme Ubp15 and the regulatory role of its terminal domains. *Biochemistry 50*, 6423−6432.

(15) Chen, J., Dexheimer, T. S., Ai, Y., Liang, Q., Villamil, M. A., Inglese, J., Maloney, D. J., Jadhav, A., Simeonov, A., and Zhuang, Z. (2011) Selective and Cell-Active Inhibitors of the USP1/ UAF1 Deubiquitinase Complex Reverse Cisplatin Resistance in Non-small Cell Lung Cancer Cells. *Chem. Biol. 18*, 1390−1400.

(16) Huang, T. T., Nijman, S. M., Mirchandani, K. D., Galardy, P. J., Cohn, M. A., Haas, W., Gygi, S. P., Ploegh, H. L., Bernards, R., and D'Andrea, A. D. (2006) Regulation of monoubiquitinated PCNA by DUB autocleavage. *Nat. Cell Biol. 8*, 339−347.

(17) Hong, L., and Fast, W. (2007) Inhibition of human dimethylarginine dimethylaminohydrolase-1 by S-nitroso-L-homocysteine and hydrogen peroxide. Analysis, quantification, and implications for hyperhomocysteinemia. *J. Biol. Chem. 282*, 34684−34692.

(18) Cleland, W. W. (1979) Statistical analysis of enzyme kinetic data. *Methods Enzymol. 63*, 103−138.

(19) Mileni, M., Johnson, D. S., Wang, Z., Everdeen, D. S., Liimatta, M., Pabst, B., Bhattacharya, K., Nugent, R. A., Kamtekar, S., Cravatt, B. F., Ahn, K., and Stevens, R. C. (2008) Structure-guided inhibitor design for human FAAH by interspecies active site conversion. *Proc. Natl. Acad. Sci. U. S. A. 105*, 12820−12824.

(20) Axley, M. J., Bock, A., and Stadtman, T. C. (1991) Catalytic properties of an Escherichia coli formate dehydrogenase mutant in which sulfur replaces selenium. *Proc. Natl. Acad. Sci. U. S. A. 88*, 8450−8454.

(21) Wang, H., Vath, G. M., Gleason, K. J., Hanna, P. E., and Wagner, C. R. (2004) Probing the mechanism of hamster arylamine N-acetyltransferase 2 acetylation by active site modification, site-directed mutagenesis, and pre-steady state and steady state kinetic studies. *Biochemistry 43*, 8234−8246.

(22) Sarkany, Z., Skern, T., and Polgar, L. (2000) Characterization of the active site thiol group of rhinovirus 2A proteinase. *FEBS Lett. 481*, 289−292.

(23) Miles, E. W. (1977) Modification of histidyl residues in proteins by diethylpyrocarbonate. *Methods Enzymol. 47*, 431−442.

(24) Soukri, A., Mougin, A., Corbier, C., Wonacott, A., Branlant, C., and Branlant, G. (1989) Role of the histidine 176 residue in glyceraldehyde-3-phosphate dehydrogenase as probed by site-directed mutagenesis. *Biochemistry 28*, 2586−2592.

(25) Gladysheva, T., Liu, J., and Rosen, B. P. (1996) His-8 lowers the pKa of the essential Cys-12 residue of the ArsC arsenate reductase of plasmid R773. *J. Biol. Chem. 271*, 33256−33260.
(26) Yang, G., Liu, R. Q., Taylor, K. L., Xiang, H., Price, J., and Dunaway-Mariano, D. (1996) Identification of active site residues essential to 4-chlorobenzoyl-coenzyme A dehalogenase catalysis by chemical modification and site directed mutagenesis. *Biochemistry 35*, 10879−10885.
(27) Venkatasubban, K. S., and Schowen, R. L. (1984) The proton inventory technique. *CRC Crit. Rev. Biochem. 17*, 1−44.
(28) Pickart, C. M., and Rose, I. A. (1986) Mechanism of ubiquitin carboxyl-terminal hydrolase. Borohydride and hydroxylamine inactivate in the presence of ubiquitin. *J. Biol. Chem. 261*, 10210−10217.
(29) Nijman, S. M., Luna-Vargas, M. P., Velds, A., Brummelkamp, T. R., Dirac, A. M., Sixma, T. K., and Bernards, R. (2005) A genomic and functional inventory of deubiquitinating enzymes. *Cell 123*, 773−786.
(30) Zhuang, Z., Johnson, R. E., Haracska, L., Prakash, L., Prakash, S., and Benkovic, S. J. (2008) Regulation of polymerase exchange between Poleta and Poldelta by monoubiquitination of PCNA and the movement of DNA polymerase holoenzyme. *Proc. Natl. Acad. Sci. U. S. A. 105*, 5361−5366.
(31) Hoege, C., Pfander, B., Moldovan, G. L., Pyrowolakis, G., and Jentsch, S. (2002) RAD6-dependent DNA repair is linked to modification of PCNA by ubiquitin and SUMO. *Nature 419*, 135−141.
(32) Stelter, P., and Ulrich, H. D. (2003) Control of spontaneous and damage-induced mutagenesis by SUMO and ubiquitin conjugation. *Nature 425*, 188−191.
(33) Zhuang, Z., and Ai, Y. (2010) Processivity factor of DNA polymerase and its expanding role in normal and translesion DNA synthesis. *Biochim. Biophys. Acta 1804*, 1081−1093.
(34) Nijman, S. M., Huang, T. T., Dirac, A. M., Brummelkamp, T. R., Kerkhoven, R. M., D'Andrea, A. D., and Bernards, R. (2005) The deubiquitinating enzyme USP1 regulates the Fanconi anemia pathway. *Mol. Cell 17*, 331−339.
(35) Oestergaard, V. H., Langevin, F., Kuiken, H. J., Pace, P., Niedzwiedz, W., Simpson, L. J., Ohzeki, M., Takata, M., Sale, J. E., and Patel, K. J. (2007) Deubiquitination of FANCD2 is required for DNA crosslink repair. *Mol. Cell 28*, 798−809.
(36) Samara, N. L., Datta, A. B., Berndsen, C. E., Zhang, X., Yao, T., Cohen, R. E., and Wolberger, C. (2010) Structural insights into the assembly and function of the SAGA deubiquitinating module. *Science 328*, 1025−1029.
(37) Faesen, A. C., Dirac, A. M., Shanmugham, A., Ovaa, H., Perrakis, A., and Sixma, T. K. (2011) Mechanism of USP7/HAUSP activation by its C-terminal ubiquitin-like domain and allosteric regulation by GMP-synthetase. *Mol. Cell 44*, 147−159.
(38) Zhang, W., Sulea, T., Tao, L., Cui, Q., Purisima, E. O., Vongsamphanh, R., Lachance, P., Lytvyn, V., Qi, H., Li, Y., and Menard, R. (2011) Contribution of Active Site Residues to Substrate Hydrolysis by USP2: Insights into Catalysis by Ubiquitin Specific Proteases. *Biochemistry 50*, 4775−4785.
(39) Cai, S. Y., Babbitt, R. W., and Marchesi, V. T. (1999) A mutant deubiquitinating enzyme (Ubp-M) associates with mitotic chromosomes and blocks cell division. *Proc. Natl. Acad. Sci. U. S. A. 96*, 2828−2833.
(40) Joo, H. Y., Zhai, L., Yang, C., Nie, S., Erdjument-Bromage, H., Tempst, P., Chang, C., and Wang, H. (2007) Regulation of cell cycle progression and gene expression by H2A deubiquitination. *Nature 449*, 1068−1072.
(41) Quesada, V., Diaz-Perales, A., Gutierrez-Fernandez, A., Garabaya, C., Cal, S., and Lopez-Otin, C. (2004) Cloning and enzymatic analysis of 22 novel human ubiquitin-specific proteases. *Biochem. Biophys. Res. Commun. 314*, 54−62.
(42) Polgar, L. (1974) Mercaptide-imidazolium ion-pair: the reactive nucleophile in papain catalysis. *FEBS Lett. 47*, 15−18.
(43) Brocklehurst, K., Watts, A. B., Patel, M., Verma, C., Thomas, E. W., and Sinnott, M. (1998) *Comprehensive Biological Catalysis: A Mechanistic Reference*, pp 381−423, Academic Press, San Diego, CA.
(44) Polgar, L. (1973) On the mode of activation of the catalytically essential sulfhydryl group of papain. *Eur. J. Biochem. 33*, 104−109.
(45) Polgar, L. (1989) *Mechanisms of Protease Action*, CRC, Boca Raton, FL.
(46) Schneck, J. L., Villa, J. P., McDevitt, P., McQueney, M. S., Thrall, S. H., and Meek, T. D. (2008) Chemical mechanism of a cysteine protease, cathepsin C, as revealed by integration of both steady-state and pre-steady-state solvent kinetic isotope effects. *Biochemistry 47*, 8697−8710.
(47) Bergmann, E. M., and James, M. N. G. (1999) in *Proteases of Infectious Agents* (Dunn, B. M., Ed.) pp 139−163, Academic Press, London.
(48) Sarkany, Z., Szeltner, Z., and Polgar, L. (2001) Thiolate-imidazolium ion pair is not an obligatory catalytic entity of cysteine peptidases: the active site of picornain 3C. *Biochemistry 40*, 10601−10606.
(49) Huang, C., Wei, P., Fan, K., Liu, Y., and Lai, L. (2004) 3C-like proteinase from SARS coronavirus catalyzes substrate hydrolysis by a general base mechanism. *Biochemistry 43*, 4568−4574.
(50) Barretto, N., Jukneliene, D., Ratia, K., Chen, Z., Mesecar, A. D., and Baker, S. C. (2005) The papain-like protease of severe acute respiratory syndrome coronavirus has deubiquitinating activity. *J. Virol. 79*, 15189−15198.
(51) Lindner, H. A., Fotouhi-Ardakani, N., Lytvyn, V., Lachance, P., Sulea, T., and Menard, R. (2005) The papain-like protease from the severe acute respiratory syndrome coronavirus is a deubiquitinating enzyme. *J. Virol. 79*, 15199−15208.
(52) Hosfield, C. M., Elce, J. S., Davies, P. L., and Jia, Z. (1999) Crystal structure of calpain reveals the structural basis for Ca(2+)-dependent protease activity and a novel mode of enzyme activation. *EMBO J. 18*, 6880−6889.